

Electronic Binding Energies and Scaling Relations for FCC Transition Metals

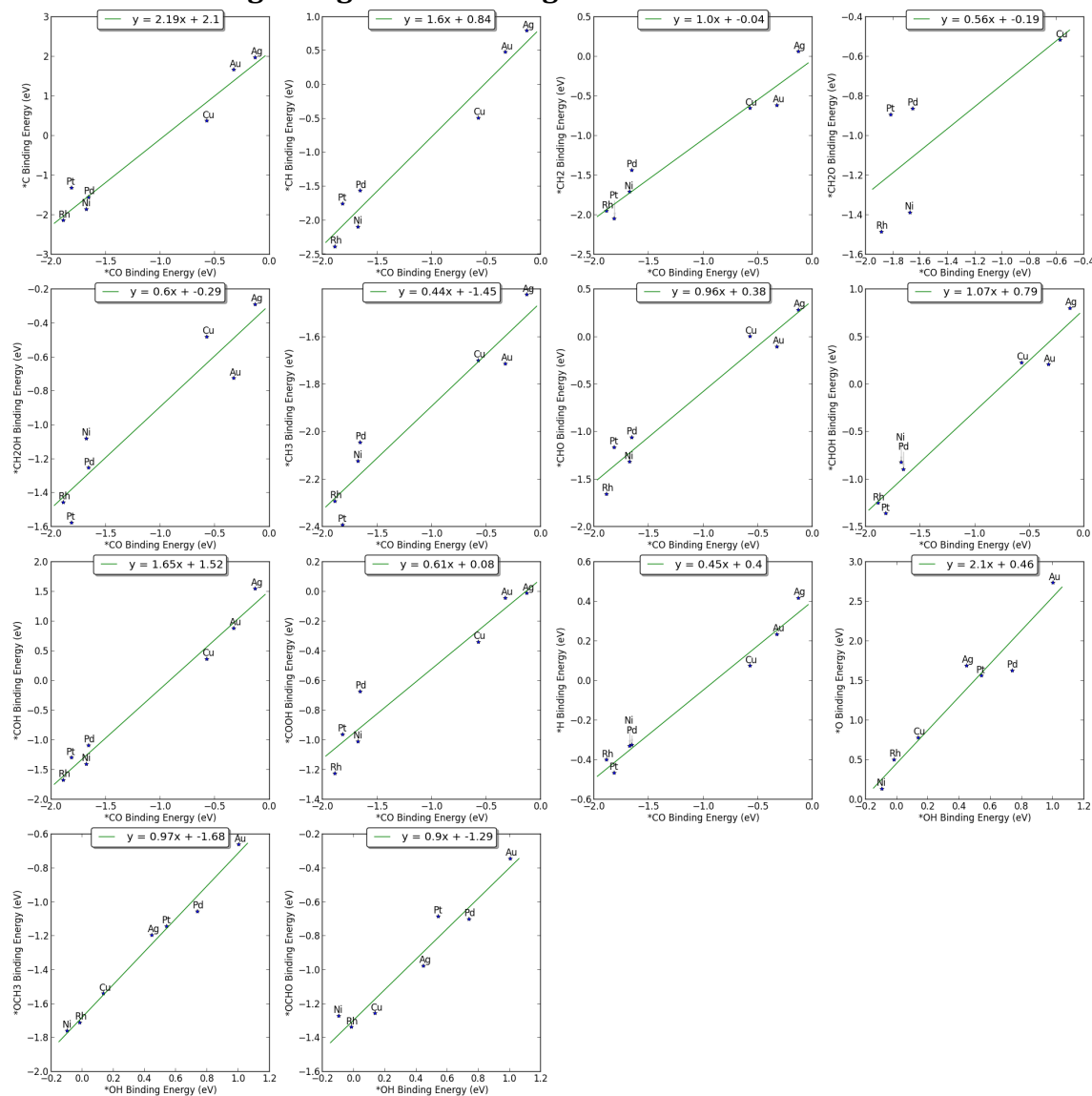


Figure S1. Scaling relations for CO₂RR intermediates on FCC(100) transition metal facets.

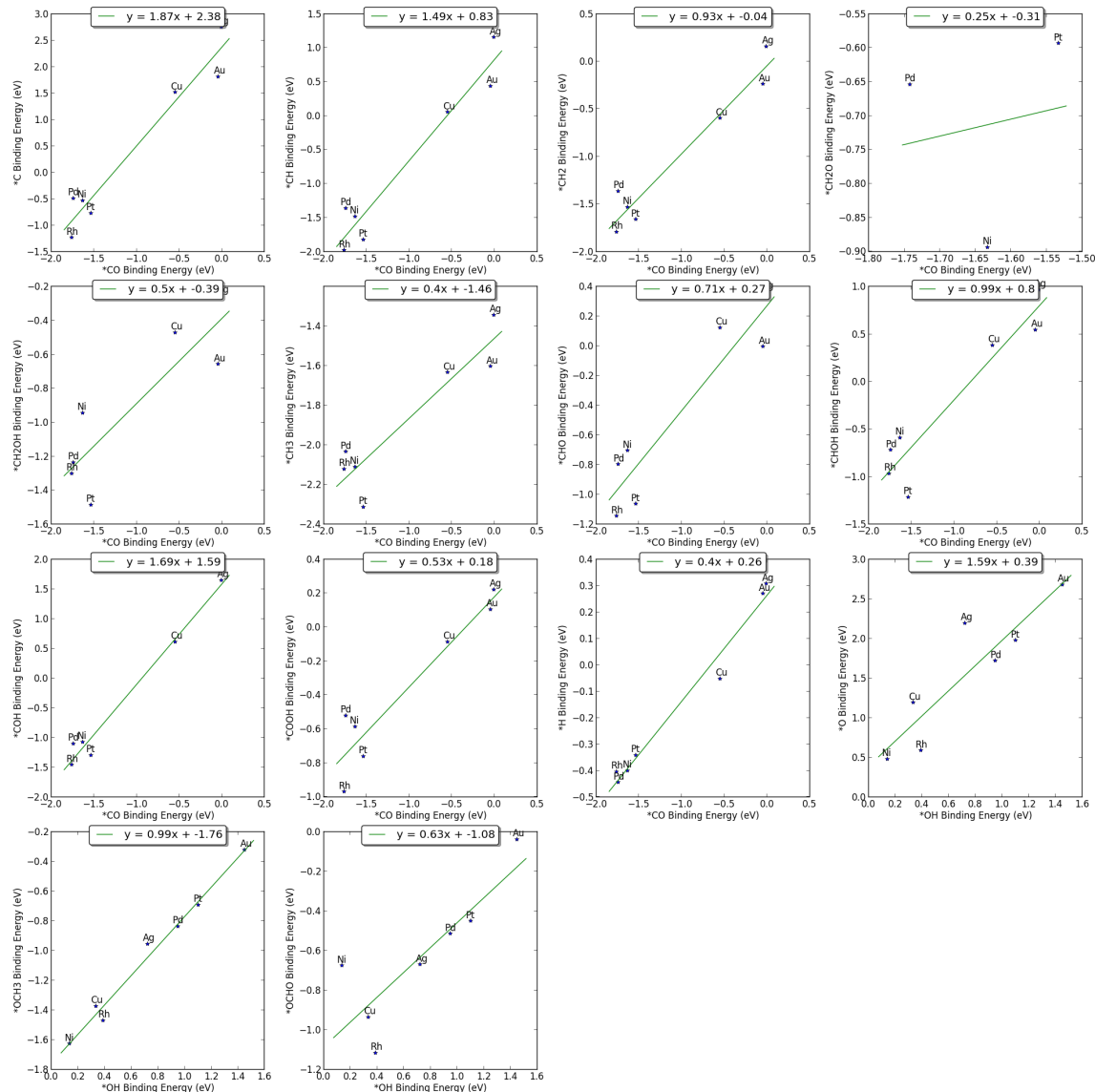


Figure S2. Scaling relations for CO₂RR intermediates on FCC(111) transition metal facets.

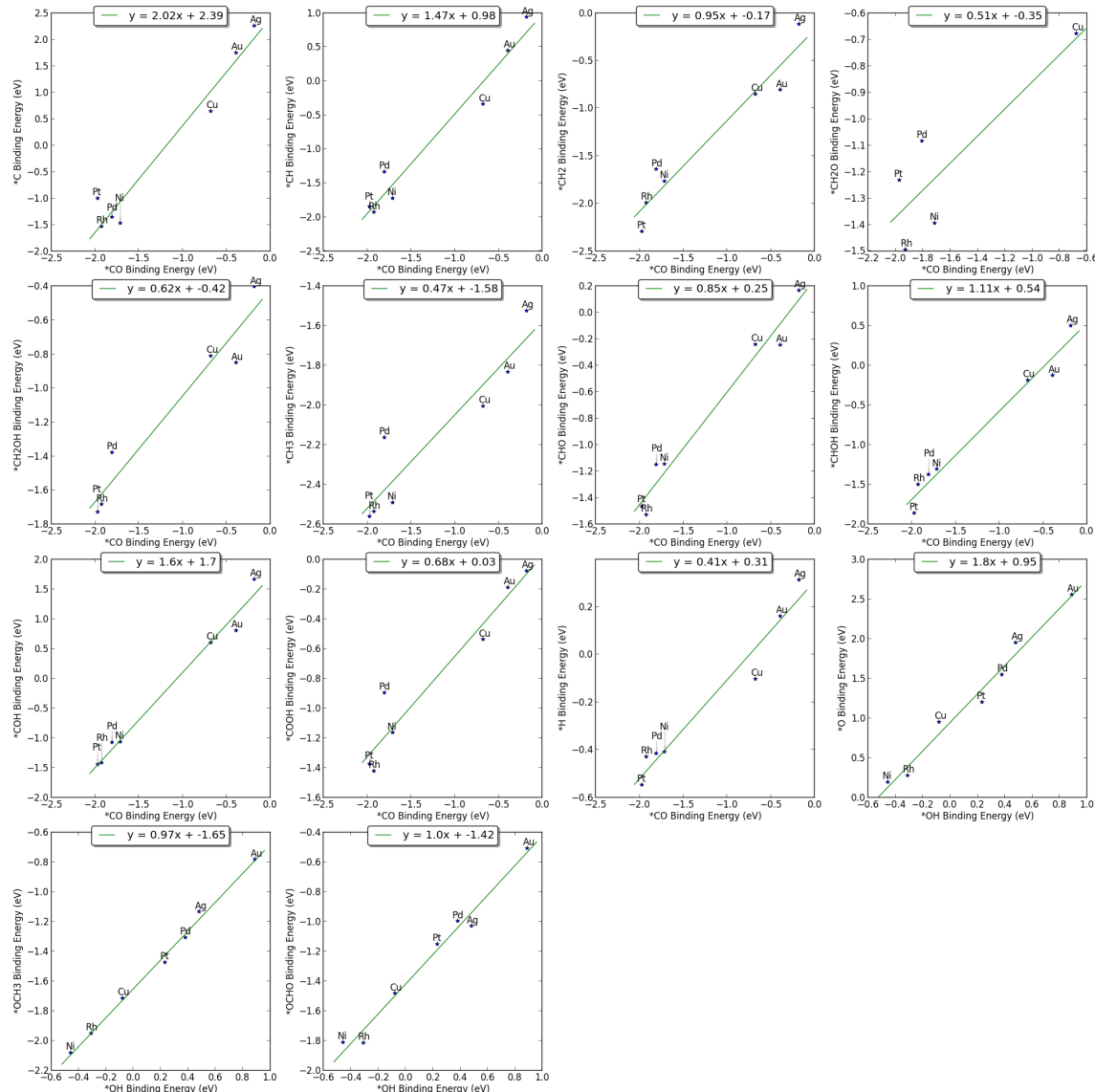


Figure S3. Scaling relations for CO₂RR intermediates on FCC(211) transition metal facets.

In Figures S1, S2, and S3, scaling relations for the electronic binding energies of 14 CO₂RR intermediates are plotted against the electronic binding energies of $^{*}\text{CO}$ or $^{*}\text{OH}$. Calculations for the (211) facet use data from the same underlying calculations as Peterson et al. (2012)¹, but numbers are reported to give a consistent reference. All electronic binding energies are referenced to formation energies based on calculations of gas phase CO, H₂O, and H₂.

Details of Binding Energies on $^{*}\text{CO}$ covered Pt(111)

Calculations for binding energies of $^{*}\text{CHO}$, $^{*}\text{COH}$, $^{*}\text{COOH}$, and $^{*}\text{H}$ on $^{*}\text{CO}$ -covered Pt(111) surface used different calculation parameters and methodology (minima hopping) than the low coverage binding energies. We summarize the calculation parameters in the table below:

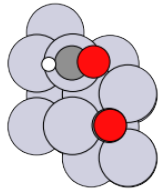
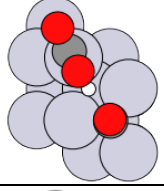
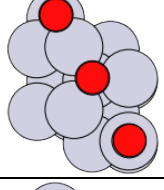
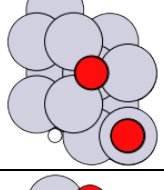
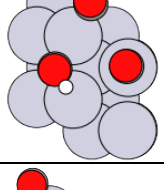
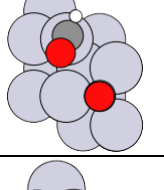
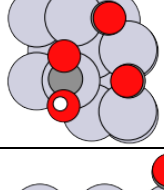
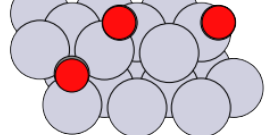
Slab Size	# of *CO Initially	Initial Coverage of *CO	Coverage of Adsorbates	k-points
2×2	0	0	0.125	6×6×1
2×2	1	0.25	0.375	6×6×1
2×2	2	0.5	0.625	6×6×1
3×2	4	0.67	0.75	4×6×1

Table S1. Table of calculation parameters for high *CO coverage calculations on Pt(111).

It is important to note that in Figure 1 of the main text, the green triangles are labeled with coverages corresponding to the “Coverage of Adsorbates” column in Table S1. In Figure 3 of the main text, the plot titles of “*CO Coverage” correspond to the “Initial Coverage of *CO” in Table S1. We find that this methodology reports a more relevant and realistic coverage that is consistent within a given figure.

For each coverage and for each adsorbate (including the no additional adsorbate case), a global optimization method^{2,3} was employed (minima hopping at 2000K initial temperature and 25 iterations) to find the global minimum. The minimum binding energy configurations, and binding energies are detailed below.

Slab Size	# of *CO initially	Additional Adsorbate	Electronic Binding Energy (eV)	Configuration
2×2	0	CO	-1.48	Hollow
2×2	0	H	-0.32	Hollow
2×2	0	COH	-1.30	Hollow
2×2	0	CHO	-1.06	Top
2×2	0	COOH	-0.76	Top
2×2	1	CO	-1.17	
2×2	1	H	-0.11	
2×2	1	COH	-0.86	

2×2	1	CHO	-0.83	
2×2	1	COOH	-0.25	
2×2	2	CO	-0.85	
2×2	2	H	-0.06	
2×2	2	COH	-0.57	
2×2	2	CHO	-0.39	
2×2	2	COOH	0.42	
3×2	4	none	0.00	

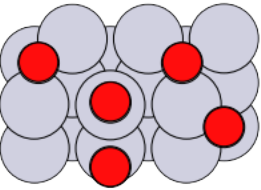
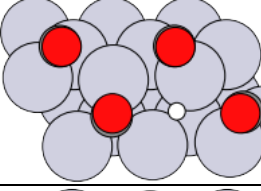
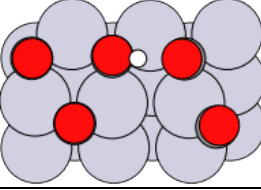
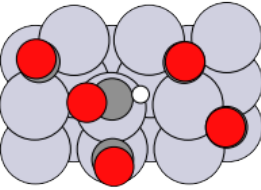
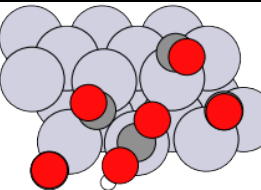
3×2	4	CO	1.06	
3×2	4	H	0.47	
3×2	4	COH	1.11	
3×2	4	CHO	0.98	
3×2	4	COOH	1.37	

Table S2. Table of electronic binding energies and minimum energy configurations for key adsorbates on *CO-covered Pt(111).

Free Energy Diagrams for CO₂ Reduction on FCC(111) Surfaces

Below, we plot free energy diagrams for the CO₂RR to single-carbon products on fcc(111) transition metal surfaces. Adsorbed *CH₂O is not stable on many of these surfaces, and gas phase "CH₂O" is used to denote surfaces for which this is the case. These diagrams show some likely paths for the CO₂RR on these surfaces, but they are not representative of every possible reaction pathway that can reach these products. For example, *CHOH shown below comes from a proton-electron transfer to the C-end of *COH, but it can also be made from a proton-electron transfer to the O-end of *CHO.

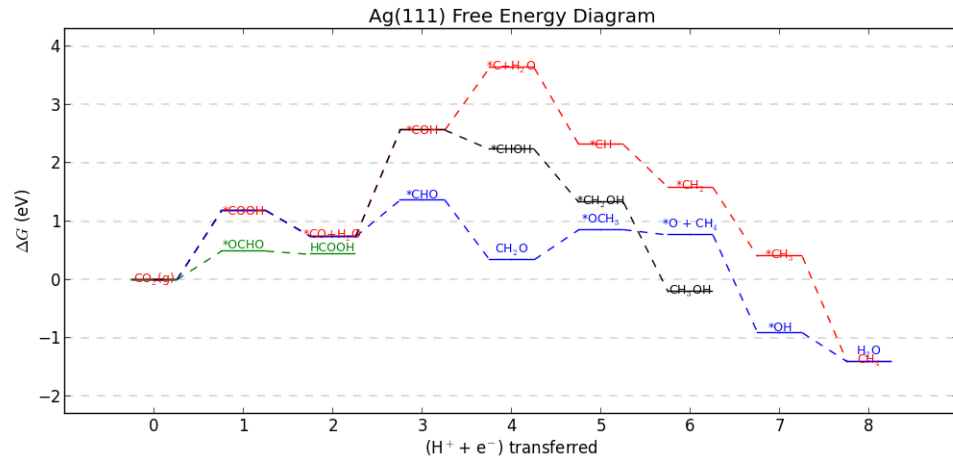


Figure S4. Free energy diagram for the CO2RR to single-carbon products on Ag(111)

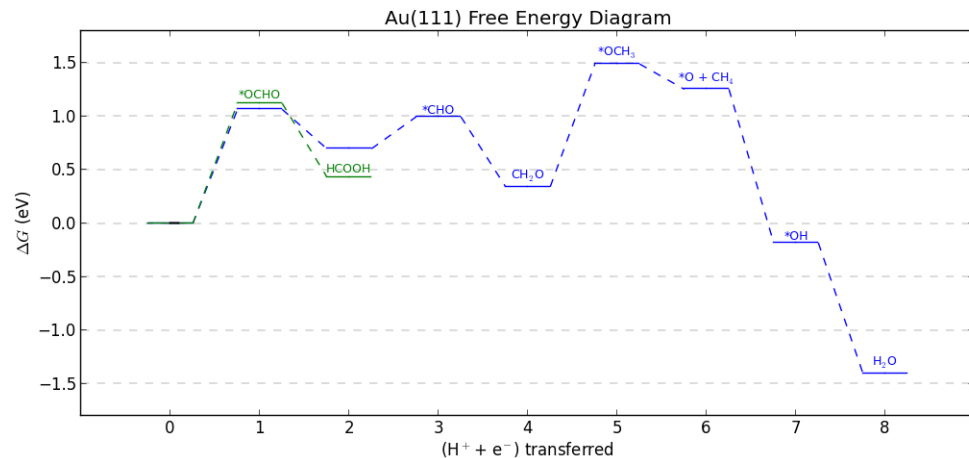


Figure S5. Free energy diagram for the CO2RR to single-carbon products on Au(111). Pathways involving *COH are inaccessible due to the instability of *COH on Au(111), which is calculated to spontaneously dissociate into *CO and *H.

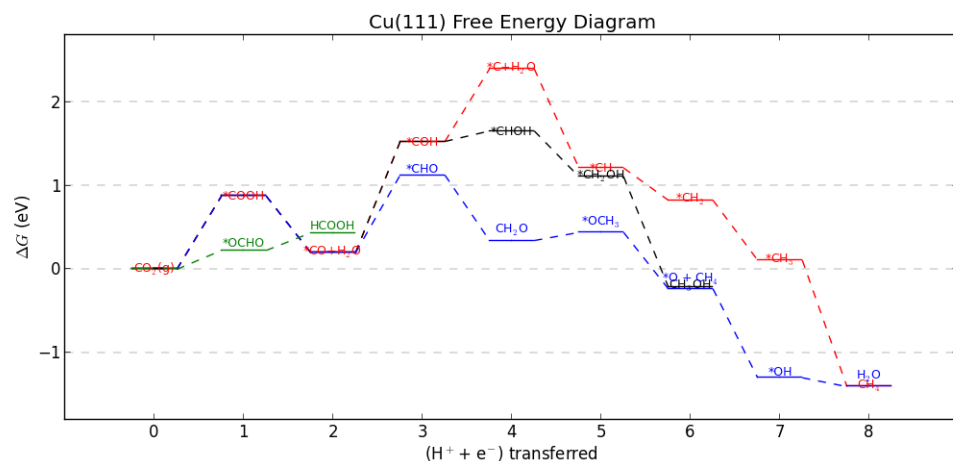


Figure S6. Free energy diagram for the CO2RR to single-carbon products on Cu(111)

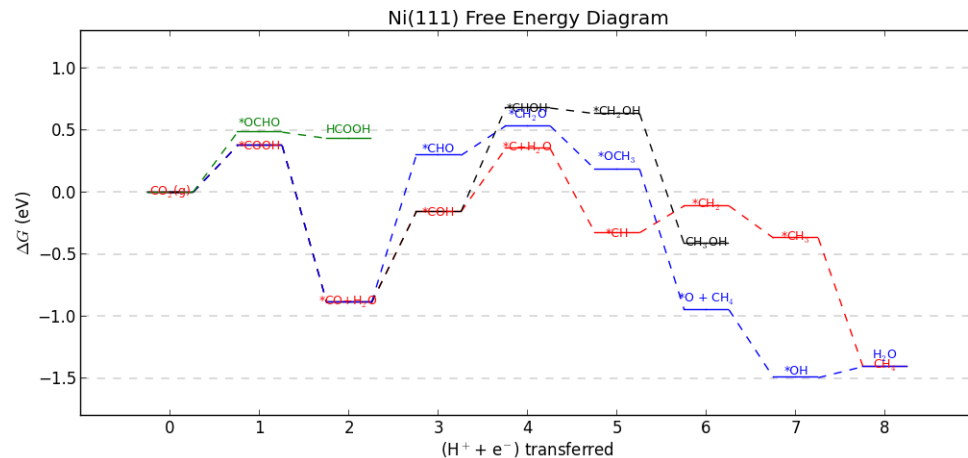


Figure S7. Free energy diagram for the CO₂RR to single-carbon products on Ni(111)

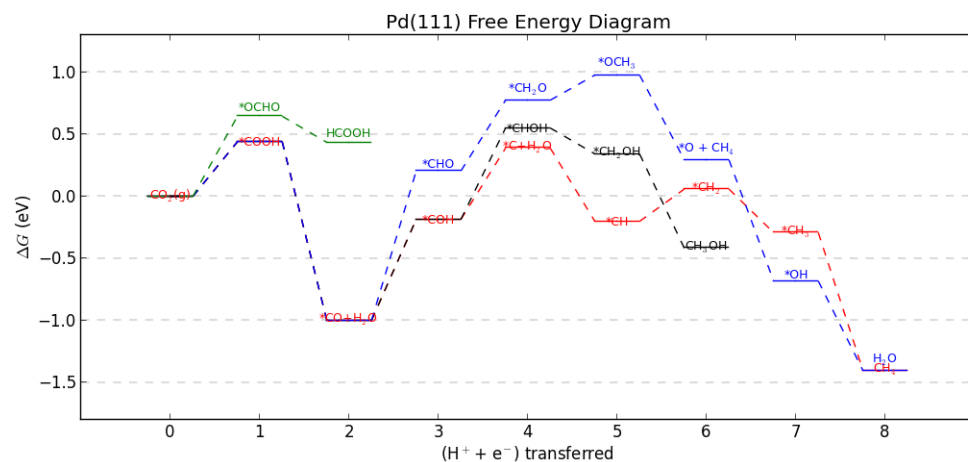


Figure S8. Free energy diagram for the CO₂RR to single-carbon products on Pd(111)

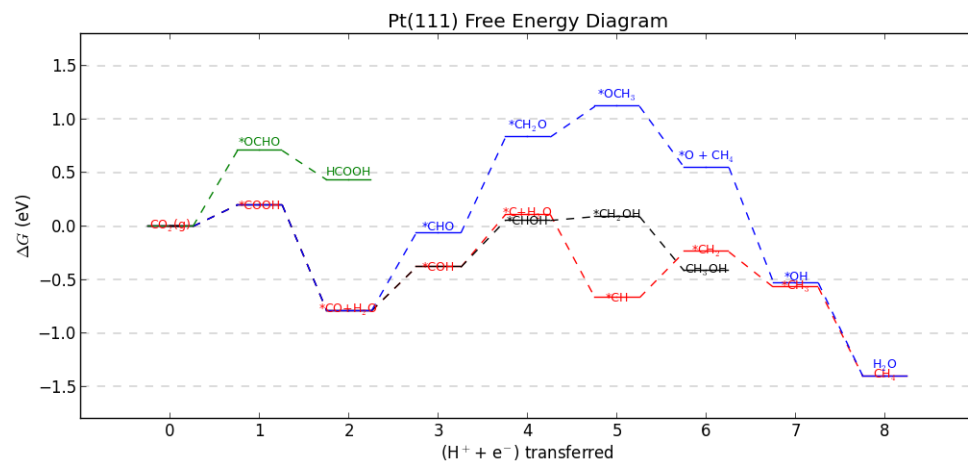


Figure S9. Free energy diagram for the CO₂RR to single-carbon products on Pt(111)

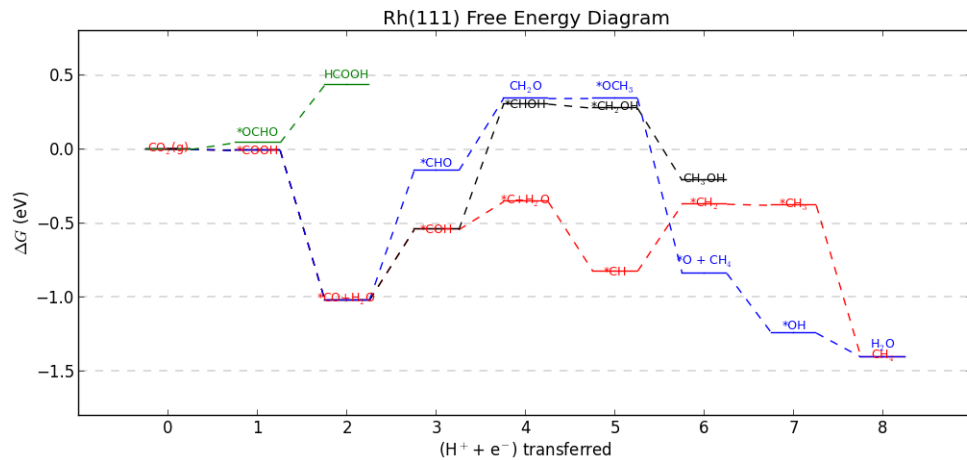


Figure S10. Free energy diagram for the CO₂RR to single-carbon products on Rh(111)

Full CO₂RR Activity Maps

For clarity, the activity maps in Figure 4 in the main paper only show elementary steps for CO₂RR that are potential-limiting at some *CO binding energy. The full activity map including all steps are shown in Figure S11.

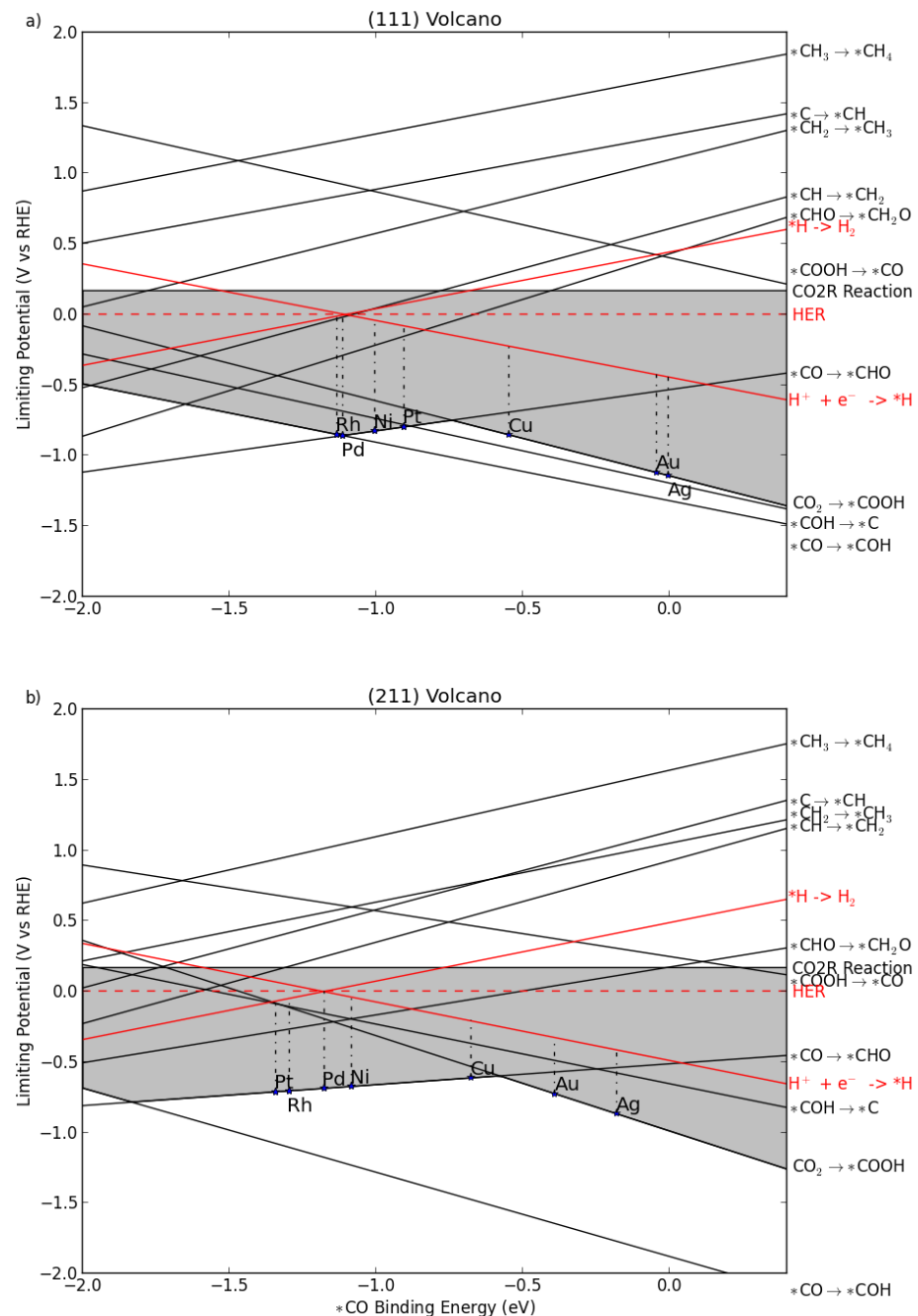


Figure S11. Full CO₂RR activity maps for the (111) and (211) facets of various fcc transition metals. Between *CO binding energies of -2.0 eV and 0.5 eV on both facets, only three steps are ever potential-limiting.

Including Adsorbate-Adsorbate Effects in Scaling Relations

As mentioned in the main text, at high *CO coverage, the binding energy of *COOH and *COH deviate from the scaling relation by a somewhat significant amount – at 0.625ML coverage, *COOH binding is weaker than the scaling would suggest by 0.39 eV and *COH binding is stronger than the scaling would suggest by 0.51 eV. We can incorporate these deviations by allowing the scaling relation themselves to shift according to the deviation (*COOH becomes less stable relative to *CO and *COH becomes more stable relative to *CO). The result of this shift is shown in the activity map below:

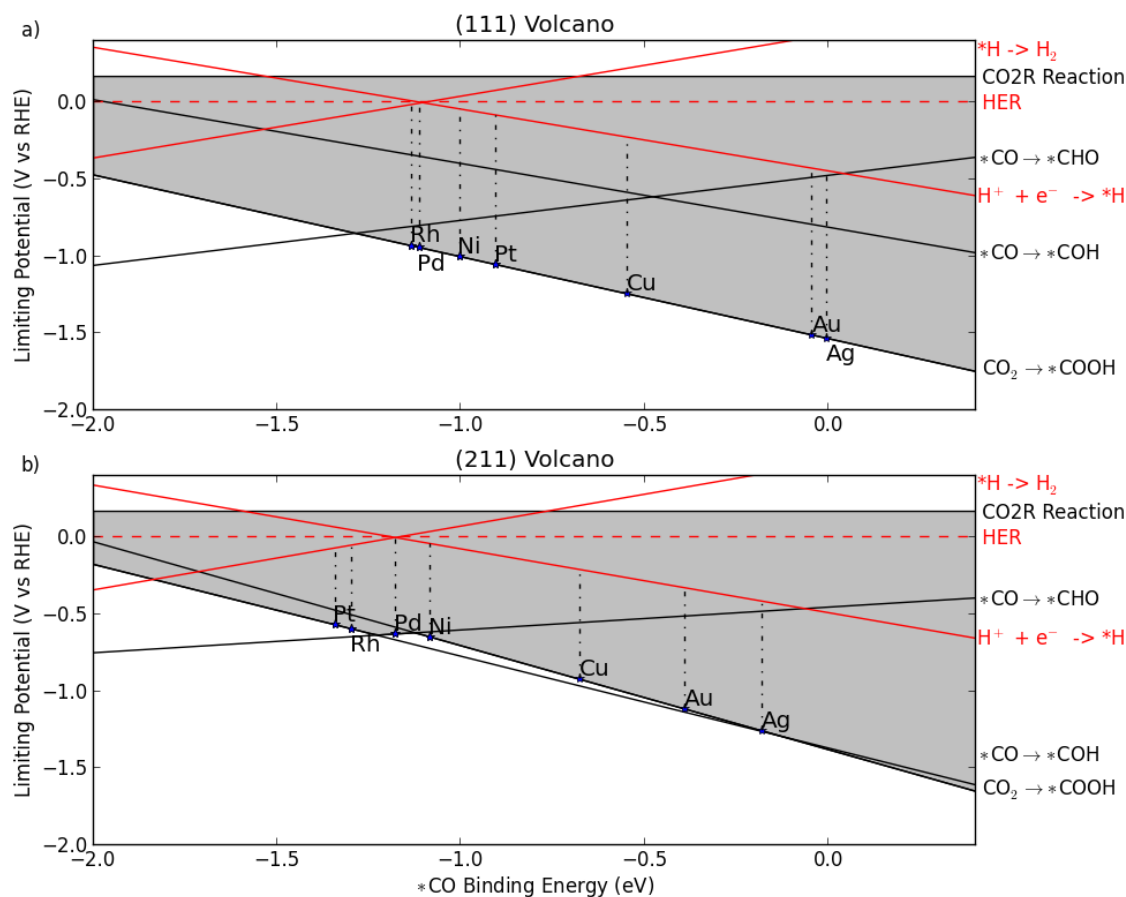


Figure S12. CO₂RR activity maps for the (111) and (211) facets of various fcc transition metals incorporating deviations from linear scaling at high *CO coverage for *COOH and *COH.

The first point to notice about Figure S12 is that Cu, Au, and Ag do not bind *CO strongly enough to obtain this high coverage, so it is unlikely they would most likely follow the activity maps shown by Figure 4. Secondly, for the (111) facet at high *CO coverage, CO₂ activation appears to be much more difficult than *CO activation to *COH. A coverage of *CO that would effect this significant of a shift would be unlikely to exist at steady state due to the difficulty of replenishing *CO from the CO₂

activation step being so heavily punished at high *CO coverage. The true picture for the CO₂RR on these strong-binding terraces lies somewhere between the extremes painted by Figure 4 and Figure S12. Limiting potentials for the (211) facets of Pt, Ni, Pd, and Rh do not change significantly.

References

1. A. A. Peterson and J. K. Nørskov, *J. Phys. Chem. Lett.*, 2012, **3**, 251–258.
2. A. A. Peterson, *Top. Catal.*, 2013.
3. S. Goedecker, *J. Chem. Phys.*, 2004, **120**, 9911–7.